scavengers and neurotrophins was tested. Previous in vitro and in vivo experiments in different systems showed that a combination of ROS scavengers and a variety of trophic agents could act synergistically (13, 21). Gabaizadeh et al. (13) demonstrated synergistic protection of auditory neurons and auditory hair cells from cisplatin ototoxicity in vitro by using a combination of an ROS scavenger and BDNF. In a study using a noise-induced model, glial cell line-derived neurotrophic factor (GDNF) effected a further reduction in threshold shifts in addition to the reduction attained with deferoxamine and mannitol (5). In contrast, a combination of NT-3 and an NMDA antagonist (MK801) was found to protect against hair cell damage as well as completely preventing the loss of 90% of the auditory neurons which occured following amikacin administration in the guinea pig model of aminoglycoside ototoxicity (22). We have also shown quite definitely that the combination of an NOS inhibitor and BDNF had a significantly stronger protective effect against GM-induced ototoxicity (23). Nevertheless, in spite of these trials, the preventive mechanisms of these drugs and a reliable method for their combination remain obscure. The aim of this study was to determine the individual efficacy of each drug and to find the most suitable combination of drugs for the prevention of hair cell damage. For this purpose, we tested the influence of each drug on the GM-induced production of NO and ROS and compared the protective effect of each drug on GM-induced hair cell damage.

MATERIAL AND METHODS

Animal dissection

Forty healthy, otomicroscopically normal, adult pigmented guinea pigs with body weights in the range 200–250 g and normal Preyer's reflex were used. The care and use of the animals, as approved by the Animal Experimentation Committee, Hiroshima University School of Medicine (permit No. F9606-028), was in accordance with the Guide to Animal Experimentation, Hiroshima University and the Committee on Research Facilities for Laboratory Animal Science, Hiroshima University School of Medicine.

All animals were anaesthetized deeply with pentobarbital and immediately decapitated. The temporal bones were quickly removed and the individual vestibular end organs were dissected in artificial perilymph (AP) containing 130.0 mM NaCl, 5.4 mM KCl and 1.25 mM $CaCl_2/2H_2O$, buffered to pH 7.2 with 5.0 mM HEPES, adjusted to 300 mOsm with glucose and equilibrated with 95% O_2/5% CO_2. The utricular macula and crista ampullares were dissected in order to expose the surface of the sensory epithelium. The cupula and otoconial membrane were then removed from the surface of the sensory epithelium. To obtain individual vestibular sensory cells, the crista ampullares and utricular macula were then incubated for 20 min in AP containing 0.25 mg/ml collagenase. Further dissociation was performed mechanically and the isolated hair cells were collected for subsequent experiments (8, 23, 24).

Simultaneous detection of NO and ROS

All the utricular maculae and isolated sensory cells were loaded with 10 μM 4,5-diaminofluorescein diacetate (DAF-2DA; Daiichi Pure Chemical Co. Ltd, Tokyo, Japan) and 20 μM dihydrotetramethylrosamine (DHTMRos; Molecular Probes, Eugene OR) in AP for 20 min at 37°C in the dark (8, 24). When necessary, 100 μM L-NAME (Biomol Research Lab. Inc., Plymouth Meeting PA) was added at the time of dye loading. After DAF-2DA and DHTMRos loading, the specimens were rinsed with AP and placed in an eight-well perfusion chamber (depth 0.5 mm, diameter 9 mm, volume 3.5 μl) (PC8R-0.5; Grace Bio-Labs Inc., Bend, OR) filled with AP for imaging (8, 24).

The specimens were viewed in a Nikon fluorescence microscope (Eclipse E600) equipped with appropriate filter sets (excitation [465–495 nm] and emission [515–555 nm] filters for DAF-2DA, excitation (510–560 nm) and emission [590 nm low pass (LP)] filters for DHTMRos or Nikon dual-band filter block F-R for both DAF-2DA and DHTMRos) (24). Fluorescence analogue images were obtained using an intensified digital colour charge-coupled device camera (C4742-95; Hamamatsu Photonics) and stored as digital images using IP Lab Spectrum software (version 3.0; Signal Analytics Corporation). After completion of each experiment, fluorescence intensities were measured and analysed from the stored digital image sequences, again using the IP Lab Spectrum software.

Specimens were then perfused with 1 mM GM (Sigma-RBI Inc., St. Louis, MO) in AP and images were obtained after 1, 5, 10, 20, 40 and 60 min. D-methionine (50 mM; Sigma-RBI), leupeptin (1 mM; Sigma-RBI) or BDNF (10 ng/ml; Pepro Tech House, London) was dissolved in AP and perfusion started 30 s before GM stimulation.

For the statistical analysis, 50 sensory cells were randomly selected from each specimen and the fluorescence intensity of each was measured at each time point. The intensity values of the 50 cells were averaged for each specimen at each time point. The grand mean was obtained by averaging the means of six to eight specimens generated for each time point. Standard errors were calculated from the means for the individual specimens. These data were analysed by a two-way ANOVA.

Protection experiments

In order to assess the GM-induced cell damage of the neurosensory epithelium, specimens were incubated either in Hank's balanced salt solution (HBSS) alone, or in HBSS containing GM (2 mg/ml; Sigma-Aldrich). Incubation lasted for up to 8 h.

As has already been reported, sensory cells incubated in HBSS remain almost completely viable for up to 4 h. Those incubated with 2 mg/ml GM were significantly damaged ($p < 0.01$) after 1 h (cell survival: 60% ± 18.6%). Viability decreased further after 2 h to 43% ± 25.4%. After 4 h of incubation with GM, viability had decreased to 18% ± 22.9% and to 3% ± 4.4% after 8 h (Fig. 1) (23). The protective effect of the drugs against the GM-induced cell damage was therefore evaluated after 4 h of incubation. For protection experiments, we used 100 μM L-NAME, 50 mM D-methionine, 10 ng/ml BDNF, 1 mM leupeptin or combinations of any 2 of these drugs. Again, we compared hair cell survival. All solutions were calibrated to pH 7.2 and 300 mOsm. The results were evaluated after 4 h.

To assess cell viability, a two-colour fluorescence cell viability assay (LIVE/DEAD Viability/Cytotoxicity Assay Kit®; Molecular Probes) was used (23). The specimens were incubated for 40 min with 2 μM calcein AM and 4 μM Ethidium homodimer-1 (EthD-1) in phosphate-buffered saline after 4 h of incubation. After staining, the specimens were rinsed with HBSS and transferred to a PC8R-0.5 eight-well perfusion chamber filled with HBSS for imaging (23).

The specimens were viewed in a Nikon fluorescence microscope (Eclipse E600) equipped with an appropriate filter set (Nikon dual-band filter block F-R). After the completion of each experiment, 50 sensory cells were randomly selected from each specimen. The numbers of living and dead cells were counted and cell survival was calculated as a percentage.

For the statistical analysis, the mean value was obtained by averaging the hair cell survival rate of six to eight specimens. Standard errors were calculated from the means for the individual specimens. These data were analysed by a two-way ANOVA.

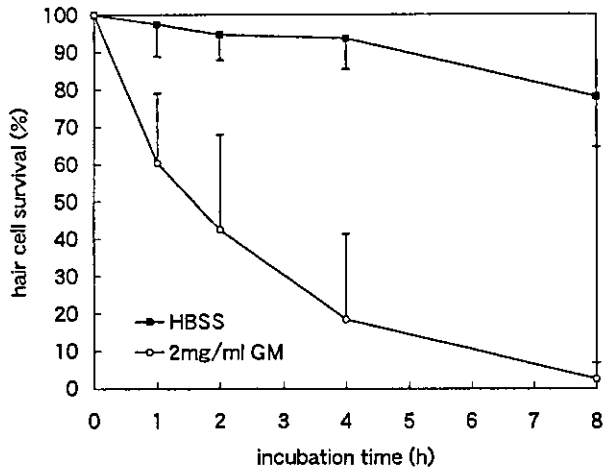

Fig. 1. Survival of isolated vestibular sensory cells incubated in HBSS with or without 2 mg/ml GM.

RESULTS

Simultaneous detection of NO and ROS

Production of NO was determined by the observation of a green-fluorescing signal following incubation with DAF-2DA. Similarly, ROS production was determined by observation of a red-fluorescing signal after incubation with DHTMRos. After addition of 1 mM GM, the green fluorescence was localized to the sensory epithelium, especially in the sensory cells and also in the blood vessels. The red fluorescence was localized mainly in the sensory cells. In contrast, there was no significant fluorescence in the surrounding tissue, i.e. the supporting cells. When the experiment was started there was only weak green fluorescence but, after adding 1 mM GM to the medium, the fluorescence intensity increased time-dependently, reaching a maximum within 40 min. Red fluorescence intensity also increased time-dependently, culminating within 20 min. A non-specific NOS inhibitor, L-NAME, inhibited the production of NO, but did not cause any significant changes in the production of ROS. Either a radical scavenger, D-methionine, or a neurotrophin, BDNF, suppressed the production of ROS. An increase in red fluorescence was suppressed and the fluorescence intensities were about half of those following stimulation with GM alone. In contrast, the production of NO was stimulated by the presence of D-methionine or BDNF. The green fluorescence intensity increased very rapidly and was higher ($p < 0.01$) than that without D-methionine or BDNF. A calpain inhibitor, leupeptin, did not produce any changes in either green or red fluorescence intensity. As a control, both green and red fluorescence intensities remained unchanged in the absence of GM stimulation (Fig. 2).

Twenty min after stimulation with GM the fluorescence intensities of NO were: 186 ± 26 (control), 227 ± 16 (BDNF), 46 ± 9 (L-NAME), 237 ± 11 (D-methionine) and 191 ± 25 (leupeptin). The fluorescence intensities of ROS were: 193 ± 10 (control), 132 ± 13 (BDNF), 181 ± 15 (L-NAME), 104 ± 3 (D-methionine) and 181 ± 5 (leupeptin) (Fig. 3).

Protective agents against GM toxicity

Co-incubation of the isolated sensory cells with L-NAME (100 μM) provided partial protection of sen-

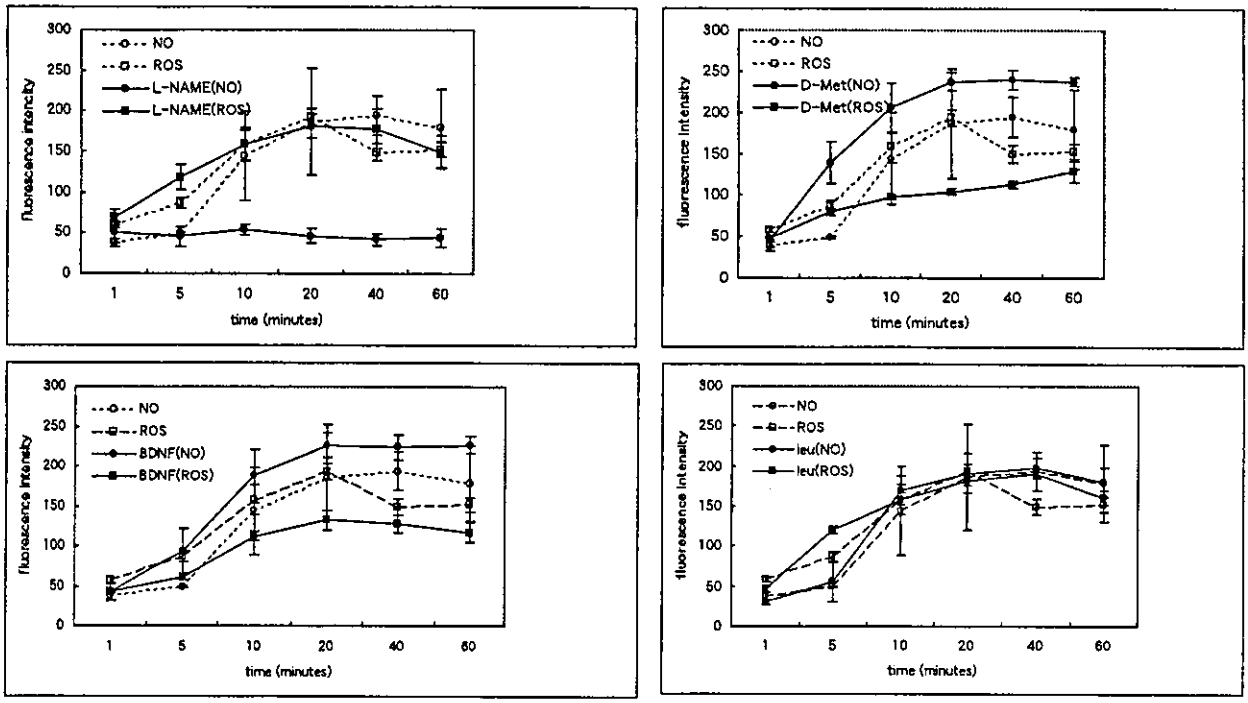

Fig. 2. Fluorescent intensity changes in vestibular sensory cells after GM stimulation, either alone or in the presence of L-NAME, D-methionine (D-Met), BDNF or leupeptin (leu).

sory cells from GM toxicity. Cell survival (56% ± 12.0%) was significantly ($p < 0.01$) better than in cells treated with GM alone. D-methionine (50 mM), BDNF (10 ng/ml) and leupeptin (1 mM) also provided partial but significant ($p < 0.01$) protection of sensory cells from GM toxicity. Survival declined to 56% ± 24.6% (D-methionine), 63% ± 20.4% (BDNF) and 60% ± 9.9% (leupeptin) after 4 h of incubation. There was no significant difference between the protective effects of these four agents. The combinations L-NAME + BDNF, L-NAME + leupeptin and D-methionine + leupeptin showed significantly stronger protective effects against GM-induced injury to the sensory cells than L-NAME, D-methionine, BDNF and leupeptin separately ($p < 0.01$). The survival values of sensory cells were 92% ± 11.6% (L-NAME + BDNF), 80% ± 18.5% (L-NAME + leupeptin) and 80% ± 11.1% (D-methionine + BDNF) after 4 h of incubation, thus showing no significant mutual differences. Neither of the combinations L-NAME + D-methionine (53% ± 25.3%) nor BDNF + leupeptin (61% ± 14.9%) showed any synergistic effect. The difference of the combination vis-à-vis that of the individual drugs was not significant (Fig. 4).

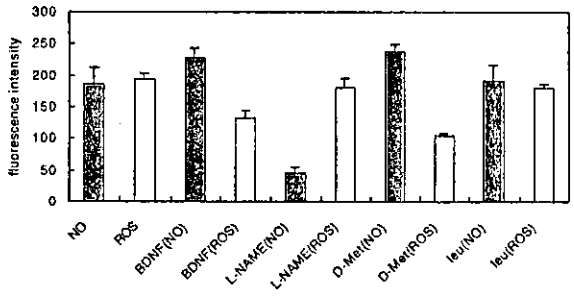

Fig. 3. Fluorescent intensity changes in vestibular sensory cells 20 min after GM stimulation, either alone or in the presence of L-NAME, D-methionine (D-Met), BDNF or leupeptin (leu).

DISCUSSION

A considerable number of studies have now been published in which hair cell damage has effectively been prevented in vivo. A variety of agents have been applied, including drugs that block NMDA receptors, calcium channel blockers, scavengers of ROS, iron chelators, corticosteroids, NOS inhibitors, neurotrophins, caspase and calpain inhibitors, etc. On the basis of previous investigations, these drugs were divided theoretically into two types. The first drug type, i.e. those blocking NMDA receptors, calcium channel blockers, ROS scavengers, iron chelators, corticosteroids and NOS inhibitors, probably works by blocking signal routes at different levels, causing

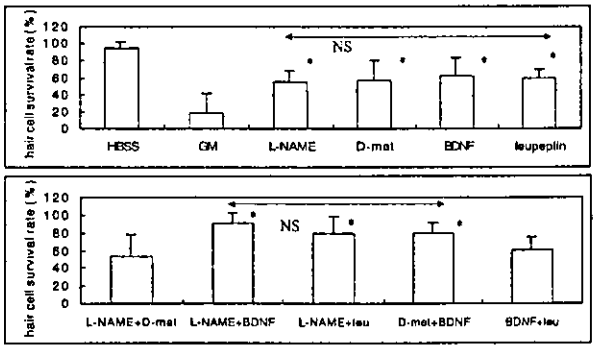

Fig. 4. Survival of isolated vestibular sensory cells incubated in HBSS with or without 2 mg/ml GM. $^{*}p < 0.01$.

oxidative stress and ultimately hair cell damage (8). The other drug type, i.e. neurotrophins and caspase or calpain inhibitors, may be closely related to the apoptotic process (16, 19, 20). All of these drugs have already been reported to protect the inner ear from damage in vivo. However, the exact preventive mechanisms of the individual drugs, as well as the effect of combinations thereof, remain unexplained. It is a well-known fact that the generation of both NO and ROS plays an important role in inner ear damage. A number of drugs that modify the NO/ROS-dependent mechanisms have been proposed to prevent inner ear damage. In this way, reduction of NO and/or ROS has been shown to afford protection from inner ear damage caused by aminoglycosides (2, 9), cisplatin (4, 10), LPS-induced labyrinthitis (6–8), acoustic trauma (5), etc.

In the present in vitro study, by using two different fluorescence indicators, DHTMRos and DAF-2DA, we have succeeded in demonstrating that the vestibular sensory cells produce both ROS and NO simultaneously following exposure to GM. As has already been reported, L-NAME inhibits the production of NO (8, 24) and D-methionine reduces the production of ROS (2, 24). This reduction of free radicals may be the main way in which these drugs attenuate the inner ear disorders caused by GM. The present study demonstrates that BDNF also inhibits the production of ROS. Several studies have now reported the beneficial effects of BDNF on the survival of compromised auditory and vestibular neurons (11–13). The mechanism by which BDNF gives protection has been speculated on but the present study indicates that the protective capacity of BDNF may in part be ascribed to the inhibition of ROS production following GM exposure, in the same way as has been shown in cisplatin-induced ROS generation (13, 24). In contrast, the calpain inhibitor leupeptin failed to inhibit the production of both NO and ROS. This means that leupeptin must prevent inner ear damage by means of some other mechanism, perhaps modulation of the apoptotic pathway (19, 20).

By using the LIVE/DEAD system, it becomes possible to evaluate the efficacy of each drug (23). All drugs used in this study provided significant protection of sensory cells against GM ototoxicity, but could not give absolute protection. Moreover, there were no significant mutual differences in survival rate. These findings may indicate that blockage of ROS alone or NO alone, or modulation of the apoptotic process only, is not sufficient to ensure complete protection. The combination L-NAME + D-methionine did not show any adjuvant effect. L-NAME inhibits NO production almost completely, whereas D-methionine gives only partial inhibition of ROS. Perhaps the volume of ROS in the presence of L-NAME and D-methionine is still sufficient to inflict some inner ear damage. Similarly, the combination BDNF + leupeptin had no adjuvant effect, indicating that blockage of the apoptotic pathway alone is also insufficient. In contrast, reduction of NO or ROS plus blockage of the apoptotic pathway (L-NAME + BDNF, D-methionine + BDNF, L-NAME + leupeptin) had a significantly stronger synergistic effect. This means that inhibition of both the free radical and the apoptotic pathway is necessary to ensure complete protection. As far as is known, GM does not directly instigate the programmed cell death process leading to apoptosis; presumably it is some initial effect of the drug inside the cell, possibly production of NO and ROS (14). It is known that NO, ROS and peroxynitrite cause apoptosis (25). Thus it is conceivable that GM initiates the production of both NO and ROS, leading to the induction of apoptosis.

The present investigation has clearly demonstrated that regulation of both the free radical pathway and the apoptotic process is necessary in order to achieve complete protection from hair cell damage. These results give us hope in our quest for new medical remedies for inner ear disorders.

ACKNOWLEDGMENTS

This study was supported by a Research Grant for Intractable Diseases (Vestibular Disorders) from the Ministry of Health, Labour and Welfare, Japan (2002), a Grant-in-Aid for Scientific Research (B)(2)(12470357) (14657437) provided by the Ministry of Education, Science and Culture, Japan and also by the Swedish Medical Research Council (grant No. 17X-7305).

REFERENCES

1. Basile AS, Huang J-M, Xie C, Webster D, Berlin C, Skolnick P. N-methyl-D-aspartate antagonists limit

aminoglycoside antibiotics-induced hearing loss. Nat Med 1996; 12: 1338–43.
2. Sha S-H, Schacht J. Antioxidants attenuate gentamicin-induced free radical formation in vitro and ototoxicity in vivo: D-methionine is a potent protectant. Hear Res 2000; 142: 34–40.
3. Garetz SL, Altschuler RA, Schacht J. Attenuation of gentamicin ototoxicity by glutathione in the guinea pig in vivo. Hear Res 1994; 77: 81–7.
4. Rybak LP, Whitworth C, Somani S. Application of antioxidants and other agents to prevent cisplatin ototoxicity. Laryngoscope 1999; 109: 1740–4.
5. Yamasoba T, Schacht J, Shoji F, Miller JM. Attenuation of cochlear damage from noise trauma by an iron chelator, a free radical scavenger and glial cell line-derived neurotrophic factor in vivo. Brain Res 1999; 815: 317–25.
6. Takumida M, Anniko M. Lipopolysaccharide-induced expression of nitric oxide synthase II in the guinea pig vestibular end organs. Eur Arch Otorhinolaryngol 1998; 255: 184–8.
7. Takumida M, Anniko M, Popa R. Possible involvement of free radicals in lipopolysaccharide-induced labyrinthitis. A morphological and a functional investigation. ORL J Otorhinolaryngol Relat Spec 1998; 60: 246–53.
8. Takumida M, Anniko M, Popa R, Zhang DM. Pharmacological models for inner ear therapy with emphasis on nitric oxide. Acta Otolaryngol 2001; 121: 16–20.
9. Takumida M, Popa R, Anniko M. Free radicals in the guinea pig inner ear following gentamicin exposure. ORL J Otorhinolaryngol Relat Spec 1999; 61: 63–70.
10. Watanabe K-I, Hess A, Bloch W, Michel O. Nitric oxide synthase inhibitor suppresses the ototoxic side effect of cisplatin in guinea pig. Anticancer Drugs 2000; 11: 401–6.
11. Lopez I, Honrubia V, Lee S-C, et al. The protective effect of brain-derived neurotrophic factor after gentamicin ototoxicity. Am J Otol 1999; 20: 317–24.
12. Zheng JL, Stewart RR, Gao WQ. Neurotrophin-4/5, brain derived neurotrophic factor, and neurotrophin-3 promote survival of cultured vestibular ganglion neurons and protect them against neurotoxicity of ototoxicins. J Neurobiol 1995; 28: 330–40.
13. Gabaizadeh R, Staecker H, Liu W, Van De Water TR. BDNF protection of auditory neurons from cisplatin involves changes in intracellular levels of both reactive oxygen species and glutathione. Mol Brain Res 1997; 50: 71–8.
14. Forge A, Li L. Apoptotic death of hair cells in mammalian vestibular sensory epithelia. Hear Res 2000; 139: 97–115.
15. Neidermeyer HP, Arnold W, Funk A, Neumann Ch, Lamm K. Apoptotic cell death in noise exposed cochlea of guinea pig. ARO Abstr 1997; 20: 479.
16. Liu W, Staecker H, Stupak H, Malgrange B, Lefebvre P, Van De Water TR. Caspase inhibitors prevent cisplatin-induced apoptosis of auditory sensory cells. Neuroreport 1998; 9: 2609–14.
17. Watanabe K, Jinnouchi K, Hess A, Michel O, Yagi T. Detection of apoptotic change in the lipopolysaccharide (LPS)-treated cochlea of guinea pig. Hear Res 2001; 158: 116–22.
18. Zheng Y, Ikeda K, Nakamura M, Takasaka T. Endonuclease cleavage of DNA in the aged cochlea of Mongolian gerbil. Hear Res 1998; 126: 11–8.
19. Cheng AG, Huang T, Stracher A, et al. Calpain inhibitors protect auditory sensory cells from hypoxia and neurotrophine-withdrawal induced apoptosis. Brain Res 1999; 850: 234–43.
20. Wang J, Ding D, Shulman A, Stracher A, Salvi RJ. Leupeptin protects sensory hair cells from acoustic trauma. Neuroreport 1999; 10: 811–6.
21. Klöcker N, Cellerino A, Bahr M. Free radical scavenging and inhibition of nitric oxide synthase potentiates the neurotrophic effects on brain-derived neurotrophic factor on axotomized retinal ganglion cells in vivo. J Neurosci 1998; 18: 1038–46.
22. Agerman K, Canlon B, Duan M, Ernfors P. Neurotrophins, NMDA receptors, and nitric oxide in development and protection of the auditory system. Ann N Y Acad Sci 1999; 884: 131–42.
23. Takumida M, Anniko M. Brain-derived neurotrophic factor and nitric oxide synthase inhibitor protect the vestibular organ against gentamicin ototoxicity. Acta Otolaryngol 2002; 122: 10–5.
24. Takumida M, Anniko M. Simultaneous detection of both nitric oxide and reactive oxygen species in guinea pig vestibular sensory cells. ORL J Otorhinolaryngol Relat Spec 2002; 64: 143–7.
25. Estevez AG, Spear N, Manuel SM, et al. Nitric oxide and superoxide contribute to motor neuron apoptosis induced by tropic factor deprivation. J Neurosci 1998; 18: 923–31.

Address for correspondence:
Masaya Takumida, MD
Department of Otolaryngology
Hiroshima University Faculty of Medicine
1-2-3 Kasumicho Minamiku
Hiroshima 734-8551
Japan
Tel.: +81 82 257 5252
Fax: +81 82 257 5254
E-mail: masati@hiroshima-u.ac.jp

in vivo *18*: 345-350 (2004)

Review

Functional Significance of Nitric Oxide in the Inner Ear

MASAYA TAKUMIDA[1] and MATTI ANNIKO[2]

[1]Department of Otolaryngology, Head and Neck Surgery, Hiroshima University Graduate School of Medicine, Hiroshima, Japan; [2]Department of Otolaryngology and Head & Neck Surgery, University Hospital (Akademiska sjukhuset), Uppsala, Sweden

Abstract. *Significant advances have been made in our understanding of the functional significance of nitric oxide (NO) in the inner ear. The localization of NO synthase and the nitric oxide production site has now been established by immunohistochemistry and the fluorescent indicator of NO. The functional significance of NO in the inner ear, especially as a neurotransmitter, is becoming increasingly clear. Mounting evidence suggests that excessive NO production may play an essential role in inner ear disorders as well. The production of an inducible type of NO synthase may be closely related to this phenomenon. Based on the mechanisms of inner ear disorders, new pharmacological strategies for preventing and/or treating inner ear disorders have also been suggested.*

Controlled production of nitric oxide (NO) plays an important role in mediating neurotransmission, regulating vascular tone and in pathophysiology. NO is synthesized by NO synthase (NOS) in an unusual reaction that converts arginine (Arg) and oxygen into citrulline and NO. Although several NOS isoforms have been isolated, all are homologous and fall into two categories with different activities and regulatory mechanisms. The constitutive neuronal (NOS I, nNOS, ncNOS) and endothelial (NOS III, eNOS, ecNOS) NOS are always present. These NOS isoforms are inactive until intracellular calcium levels increase, the calcium-binding protein calmodulin binds to calcium and the calcium - calmodulin complex binds to and activates NOS. The constitutive types of NOS (cNOS) synthesize small amounts of NO until calcium levels decrease. This intermittent production of small amounts of NO transmits signals.

In contrast, the inducible NOS isoform, NOS II (iNOS), is usually absent, but can be synthesized by virtually any cell type when adequately stimulated with cytokines or some other agent. Once produced, it invariably synthesizes large amounts of NO. The continuous production of a large quantity of NO kills or inhibits pathogens.

Recent evidence suggests that NO may play a significant role in the inner ear. Recent years has seen important advances in our understanding of the action of NO in the inner ear, not only in normal but also under pathological conditions, which this review summarizes and evaluates.

Functional significance of NO in the inner ear

Constitutive isoforms of NOS (NOS I and III). In the inner ear, constitutive isoforms of NOS (NOS I and III) have recently been identified both in the cochlea and in the vestibular end organs, mainly by using NADPH-diaphorase histochemistry and immunohistochemistry (1-5). In the organ of Corti, NOS I was localized in the nerve fibres of the spiral ganglion itself, spiral ganglion cells, the nerve fibres, nerve endings below the inner and outer hair cells, the inner and outer hair cells, Deiters' cells, pillar cells, stria vascularis and spiral ligament (1,2,4,5). In the vestibular end organs, *i.e.* crista ampullares, utricular and saccular maculae, NOS I was localized in the vestibular ganglion cells, nerve fibres, the cytoplasm of both type I and type II sensory cells, the nerve fibres contacting the type II cells, dark cells and transitional cells (2, 3).

In the cochlea, NOS III was localized in the nerve fibres of the spiral ganglion, the spiral ganglion cells, the nerve fibres, nerve endings below the inner and outer hair cells, the inner and outer hair cells, Deiters' cells, pillar cells, stria vascularis, spiral ligament, the endothelium of blood vessels

Correspondence to: Masaya Takumida, Department of Otolaryngology, Hiroshima University School of Medicine, 1-2-3 Kasumicho, Minamiku, Hiroshima 734-8551, Japan. e-mail: masati@hiroshima-u.ac.jp

Key Words: Inner ear, nitric oxide, reactive oxygen species, pathology, Meniere's disease, review.

0258-851X/2004 $2.00+.40

below the basilar membrane, the surrounding small capillaries in the lateral wall tissue and strial capillaries (1, 2, 4, 5). In the vestibular end organs, NOS III was localized in the vestibular ganglion cells, nerve fibres, the cytoplasm of both type I and type II sensory cells, the nerve fibres contacting the type II cells, dark cells, transitional cells and blood vessels in the subepithelial tissues (2,3).

As in many other organ systems, NO also plays an important role in the inner ear to regulate physiological reactions in both the cochlea and vestibular parts of the labyrinth. With regard to the effects of NO on neurotransmission, there is general consensus that NOS inhibitors may inhibit (and NO donors may facilitate) the electrical activity of afferent neurons. NO significantly contributes to the basal discharge and to the response of afferent fibres to mechanical stimuli. NO from the post-synaptic neurons binds to the N-methyl-D-aspartic acid (NMDA) receptor. NO acts directly on a side of the receptor channel complex such as the redox modulatory side. NO binding on the redox modulatory side reduces the activity of the NMDA receptor (6). In the organ of Corti, a negative feed-back mechanism has been suggested. Excitation of inner hair cells causes liberation of glutamate, which stimulates NMDA-type receptors on the afferent synaptic terminal. In addition, stimulation of the NMDA receptor liberates NO, which diffuses out of the synaptic terminal and inhibits the NMDA receptor (negative feedback mechanism). This hypothesis is supported by the finding that iontophoretically applied L-N^G-nitroarginine methylester (L-NAME), a potent NOS inhibitor, augmented the NMDA and α-amino-3-hydroxy-5-methyl-4-isoxazole propionic acid (AMPA)-induced increase in afferent fibre activity (1, 7).

NO produced in an efferent button could increase synaptic transmission in the hair cells contacted by the button, but NO produced in a hair cell could only increase transmission in neighbouring hair cells and not in the same hair cell (8). NOS-containing efferents release NO in the periphery. This in turn would stimulate the afferents into which they feed. Thus efferents acting on hair cells in the periphery would produce a type of positive feedback on both the afferents and the hair cells.

Compelling physiological evidence supports a role for the inner ear NO in the regulation of cochlear and vestibular blood flow. Round window membrane application of NO donors increases cochlear and vestibular blood flow (9). Conversely, the NOS inhibitor L-NAME reduces cochlear blood flow (10). The observed decrease of cochlear blood flow was presumably the result of a decrease in NO production, which was confirmed in the current study of isolated cochlear vascular endothelium (11). These data strongly suggest that NO production from cochlear and vestibular vessels actively regulates blood flow. Furthermore, recent data suggest that even under pathological conditions, such as acute focal cochlear microcircular disorder, formation of endogenous NO plays a key role in maintaining the cochlear blood flow (12).

Inducible type of NOS (NOS II)

NOS II has not been detected in the normal inner ear in general. This inducible type of NOS was first recognized in the vestibular epithelia by Takumida and Anniko (13) after intratympanic injection of lipopolysaccharide (LPS). The expression of NOS II in the inner ear has been further confirmed under pathological conditions such as following inoculation of LPS (14,15), gentamicin (16) and cisplatin (17), into the hydropic ear (18,19), in ageing (20), following immune response (21), *etc.* and may play an essential role in pathological damage of the inner ear (22).

Under pathological conditions, NOS II was localized in inner and outer hair cells representing nerve fibres and synaptic nerve endings, phalangeal dendrites of Deiters' cells pointing to the cuticular membrane, Hensen's cells, the cells lining scala tympani, the stria vascularis, nerve fibres, spiral ganglion cells, *etc.* in the cochlea. In the vestibular end organs, NOS II is induced in the cytoplasm of both type I and type II cells, dark and transitional cells, the nerve fibres and vestibular ganglion cells (13-22).

Direct detection of NO production site

There are two general approaches to the investigation of NO-producing sites. One possible way is to investigate the localization of NOS by using NADPH-diaphorase histochemistry or immunohistochemistry for NOS, instead of direct detection of NO. Recently, Kojima *et al.* (23,24) reported a useful method for real-time analysis of intracellular NO in living smooth muscle cells by using 4,5-diaminofluorescein diacetate (DAF-2DA). This compound, an ester, is cell permeable and is hydrolyzed by intracellular esterase, generating 4,5-diaminofluorescein (DAF-2). DAF-2 is a new fluorescent indicator of NO. Green-fluorescent triazolofluorescein (DAF-2 T), formed by reacting NO with DAF-2, is highly sensitive to NO (detection limit: 5 nM). The fluorescence in the cells increased in proportion to the concentration of NO. We have successfully applied this method to detect NO in the inner ear *in vitro* (25, 26). The results clearly indicate that NO is produced in the vestibular sensory cells, dark cells, hair cells in the organ of Corti, stria vascularis and supporting cells of the organ of Corti, *etc.* Furthermore, it has been stated that NO is produced mainly by a constitutive type of NOS in normal animals (25, 26). This assay system is useful for continuous surveillance of intracellular NO dynamics in *in vitro* systems, *e.g.* isolated vestibular end organ, isolated organ of Corti, isolated

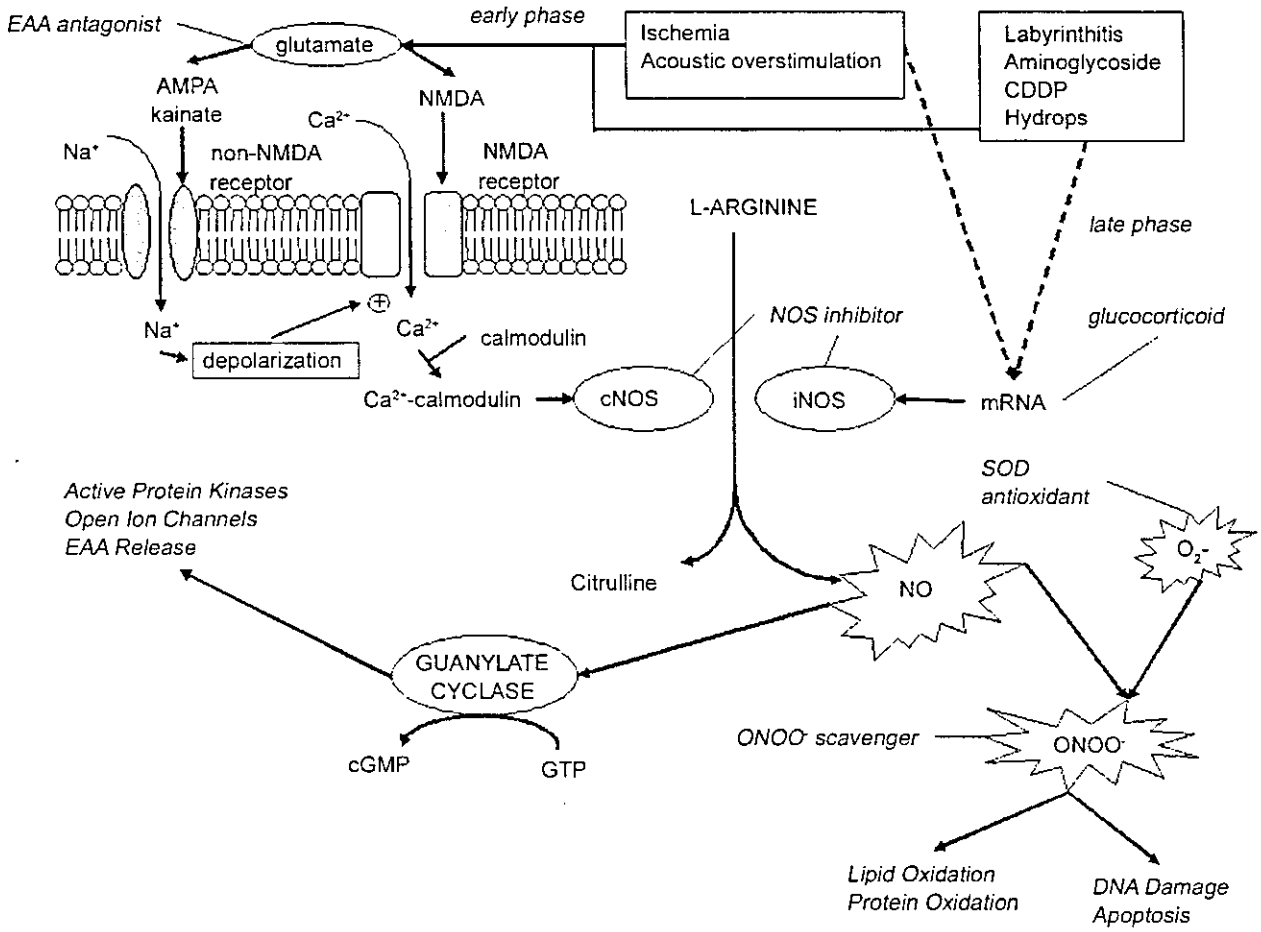

Figure 1. *Schematic diagram illustrating the production and effects of NO.*

vestibular and cochlear hair cells, *etc*. However, some problems remain when it is applied to cells located within tissues or organs, or when two types of NO-producing cells are in close proximity. In this case, it is very difficult to separate the fluorescence signals from neighbouring cells, even with a confocal laser scanning microscope. Recently, it has been stated that tissues loaded with DAF-2DA show intense fluorescence when fixed in paraformaldehyde or glutaraldehyde (27). This allows us to detect intracellular NO in fixed cells. Consequently, we assessed the procedures for detecting intracellular NO by using DAF-2DA and glutaraldehyde in the guinea pig inner ear (28). The results revealed that the combination of glutaraldehyde fixative with DAF-2DA allows us to observe intracellular NO production sites even in fixed material. In fact, we can investigate NO production sites more precisely. NO was produced in a variety of cells in the inner ear. Basically, NO-producing cells are identical to NOS-immunopositive cells. According to the results from DAF-2DA histochemistry, both vestibular and cochlear hair cells can produce NO. This has been also suggested by an DAF-2DA study using isolated vestibular and cochlear hair cells (25, 26).

NO production under different conditions

In order to establish the possible role of NO in pathological conditions, the production of NO under different conditions was investigated by using DAF-2DA.

In normal conditions, NO was produced in different types of cells such as sensory cells in the vestibular end organs, inner and outer hair cells in the organ of Corti, *etc*. After adding 1 mM L-Arg to the medium, NO from the organ of Corti and utricular maculae increased time-dependently to a maximum within 40 minutes. This increase could be suppressed by both a non-specific NOS inhibitor, L-NAME and a specific inhibitor for NOS I, 7-nitroindazole (7-NI) , but was not inhibited by a specific inhibitor of NOS II, S-ethylisothiourea (EIT). These findings may indicate that NO

is produced mainly by a constitutive type of NOS in normal animals (25, 26). Application of glutamate, NMDA, AMPA, gentamicin or LPS also increased the production of NO. These increases could be suppressed by both L-NAME and (+)-5-methyl-10,11-dihydro-5H-dibenzo [a,d] cyclohepten-5,10-imine maleate (MK801) (22, 29).

Isolated inner and outer hair cells and vestibular sensory cells were also used to confirm the suspected production of NO in the sensory cells. After addition of L-Arg, glutamate, NMDA, AMPA, or gentamicin, NO was produced from the sensory cells, while there was no significant production in the surrounding tissue, *i.e.* supporting cells (22, 25, 26, 29).

In the pathological, NOS II-induced animals, the production of NO significantly and rapidly increased to reach a maximum within 20 minutes. This increase was suppressed by EIT, while less inhibited by 7-NI, indicating that an increase in NO production in the pathological condition could be due to the expression of NOS II in the inner ear (25, 26).

Possible role of NO in pathophysiology of inner ear

Evidence has been gathered that NO might well play a role in the pathophysiology of the inner ear. From continuing investigations, a working hypothesis of otoneurotoxicity has been modelled (Figure 1) (22). Under pathological conditions, NO from a cNOS and its related excitotoxicity may mediate ototoxicity in the early phase, whereas NO from NOS II may contribute to the late phase of tissue damage in the inner ear. At NMDA receptors, glutamate triggers the opening of cation-permeable channels in the sensory cells. Extracellular Ca^{2+} could pass through the hair cell membrane *via* the voltage-dependent Ca^{2+} channels, concomitant with depolarization induced by activation of AMPA/kainate receptors. The entry of Ca^{2+} through these channels into cells stimulates NOS activity by binding to calmodulin, which is a co-factor for NOS. Actually, in the inner ear, application of glutamate and NMDA caused a rapid but transient increase in intracellular calcium concentration in a dose-dependent manner. This NO production is confirmed *in vitro* using DAF-2DA (29). After glutamate was added to the medium, the NO production of the utricular maculae and Corti's organ increased. Again, this increase could be suppressed with L-NAME. Application of NMDA or AMPA also induced an increase in NO production, though only about half of that after stimulation with glutamate. A specific non-competitive NMDA antagonist, MK-801, blocked the response to glutamate. When the AMPA antagonist 6,7 dinitroquinoxaline-2,3-dione (DNQX) was perfused, the glutamate response was similarly inhibited, though less than by MK801 (29). The synthesis of NO by NOS mediates the effects of the NMDA, quisqualate/AMPA, and kainate receptor subtypes. This involvement of NO in the early phase has also been confirmed after stimulation by LPS (22) and gentamicin (30) as well as cochlear injury induced by transient focal anoxia (31).

In a late phase of tissue damage, however, NO from NOS II may exacerbate the tissue damage. Recently, expression of NOS II has been demonstrated in the inner ear as described above. It is a well known fact that, once induced, NOS II can produce larger amounts of NO for prolonged periods of time. Prolific NO production by inner ear NOS II-positive cells can damage adjacent tissues. The significant increase in NO production in pathological animals may support the hypothesis that, even in the inner ear, NOS II is actually expressed following adequate stimulus, resulting in a profuse production of NO, which may also be involved in diseases of the inner ear (14-22).

A major action of NO is its activation of guanylate cyclase, which stimulates the production of cyclic GMP. Excess cyclic GMP depresses electric coupling, increases the spontaneous firing rate of neurons and stimulates further excitatory amino acid (EAA) release. Considerable attention has been paid recently to the rapid reaction of NO in aqueous solution with superoxide anion, yielding peroxynitrite. The direct toxicity of NO is modest but is greatly potentiated by reacting it with superoxide to form peroxynitrite. The increased accumulation of nitrotyrosine in the inner ear indicates generation of peroxynitrite in the pathological process (32-34). It can therefore be concluded that increased production of NO (from cNOS in early phase and from NOS II in late phase) and subsequent generation of peroxynitrite may be important factors responsible for the injury of the inner ear.

Neuropharmacology

If the activation of NO-dependent mechanisms is blocked by appropriate inhibitors or scavengers, then the inner ear is protected from the degenerative process (22). Actually, a number of drugs that modify NO-dependent mechanisms have been proposed for prevention of inner ear damage. Reactive oxygen species (ROS) scavengers and glutamate antagonists have been shown to provide protection from cochlear disruption by cisplatin, aminoglycoside, noise and ischemia/reperfusion injuries (35-37). Inner ear damage in the inflammatory process is also blocked by ROS or glutamate antagonists. Furthermore, such damage is also prevented by NOS inhibitors or scavengers of peroxynitrite (38-43). In our experiments in the guinea pig, intratympanic injection of bacterial LPS impaired caloric responses and caused severe and widespread morphological damage to vestibular end organs. These effects could be blocked with L-NAME, a competitive inhibitor of NOS, by applying superoxide dismutase, an O_2^- scavenger, with dexamethasone,

and with ebselen, a scavenger of peroxynitrite. Scanning electron microscopic study revealed that the ototoxic effects of gentamicin could be blocked with L-NAME, superoxide dismutase, and with ebselen (38). Exotoxin A, produced by *Pseudomonas aeruginosa*, penetrates from the middle ear into the cochlea and causes sensorineural hearing loss. The hearing impairment detected by ABR was successfully blocked by applying L-NAME (39).

Clinical application of radical scavenger

As has been described above, free radicals may play an important role in inner ear disorders and free radical scavengers can be used not only for prevention but also for treatment of inner ear disorders (22, 44). Concerning Ménière's disease, Horner and Guilhaume (45) suggested that oxidative insult probably contributes to the pathology associated with endolymphatic hydrops and that free radical scavengers might be useful in the treatment of Ménière's disease patients. In addition, Shinomori and Kimura (46) reported that allopurinol, a xanthine oxidase inhibitor and free radical scavenger, may attenuate endolymphatic hydrops and cell damage by preventing the formation of free radicals or scavenging free radicals. These findings may lead to a new approach for the treatment of Ménière's disease. Based on these results, we carried out a pilot study to determine whether radical scavenger could be used to treat Ménière's disease patients who fall into the "poor prognosis" category, *i.e.* those who do not respond to conventional medical treatment. Radical scavengers, *i.e.* rebamipide (300mg/day), vitamin C (600mg/day) and/or glutathione (300mg/day) were given orally for at least 8 weeks to 25 patients with poorly controlled Ménière's disease. After radical scavenger therapy, 21 out of 22 patients showed marked improvement of vertigo. Twelve out of 27 ears showed improvement of hearing disorders. Seventeen out of 27 ears showed improvement of tinnitus. Eighteen of 25 patients showed improvement of disability. From these results, it has been suggested that treatment using radical scavengers could potentially become an effective new therapy for Ménière's disease (47).

Conclusion

Significant advances have been made in our understanding of the functional significance of NO in the inner ear. NO acts as an important neurotransmitter and may play an important role in the regulation of inner ear blood flow. A number of studies now suggest that NO plays an essential role in the pathophysiology of the inner ear. These include aminoglycoside and cisplatin ototoxicity, acoustic trauma, inflammation, immune response, endolymphatic hydrops, ageing, *etc*. Based on these results, new pharmacological strategies can be devised to prevent and/or treat inner ear disorders. Finally, the study to elucidate the functional significance of NO in the inner ear is still proceeding and will give us greater insight into forms of treatment for hearing and vestibular disorders.

Acknowledgements

This study was supported by the Swedish Medical Research Council (grant no 17X-7305), a Health and Labor Science Research Grant for Research on Specific Disease (Vestibular Disorders) from the Ministry for Health, Labor and Welfare, Japan (2003), and Grants-in-Aid for Scientific Research (B)(2)(15390519) and (14657432) provided by the Ministry of Education, Science and Culture, Japan.

References

1 Franz P, Hauser-Kronberger.C, Böck P, Quint C and Baumgartner WD: Localization of nitric oxide synthase I and III in the cochlea. Acta Otolaryngol (Stockh) *116*: 726-31, 1996.
2 Hess A, Bloch W, Arnold S, Andressen C, Stennert E, Addicks K and Michel O: Nitric oxide synthase in the vestibulocochlear system of mice. Brain Res *813*: 97-102, 1998.
3 Takumida M and Anniko M: Localization of nitric oxide synthase isoforms (NOS I, II and III) in the vestibular end organs of the guinea pig. ORL *60*: 67-72, 1998.
4 Fessenden JD, Coling DE and Schacht J: Detection and characterization of nitric oxide synthase in the mammalian cochlea. Brain Res *668*: 9-15, 1994.
5 Gosepath K, Heinrich UR, Ecke U, Maurer J, Amedee R and Mann WJ: Possible role of nitric oxide in the physiology and pathophysiology of the guinea pig cochlea. Eur Arch Otorhinolaryngol *257*: 418-424, 2000.
6 Choi YB and Lipton SA: Redox modulation of the NMDA receptor. Cell Mol Life Sci *57*: 1534-1541, 2000.
7 Heiniger-Bürki CB, Ehrenberger K and Felix D: Is nitric oxide involved in inner ear neurotransmission? Prim Sensory Neuron *1*: 41-46, 1995.
8 Lysakowski A and Singer M: Nitric oxide synthase localized in a subpopulation of vestibular efferents with NADPH diaphorase histochemistry and nitric oxide synthase immunohistochemistry. J Comp Neurol *427*: 508-521, 2000.
9 Arenberg JG, Komjathy DA, Seidman MD and Quirk WS: Local effects of nitric oxide on vestibular blood flow in the Mongolian gerbil. Eur Arch Otorhinolaryngol *254*: 367-371, 1997.
10 Brechtelsbauer PB, Nuttall AL and Miller JM: Basal nitric oxide production in regulation of cochlear blood flow. Hear Res *77*: 38-42, 1994.
11 Shi X, Ren T and Nuttall AL: Nitric oxide distribution and production in the guinea pig cochlea. Hear Res *153*: 23-31, 2001.
12 Nagura M, Iwasaki S, Mizuta K, Mineta H, Uemura K and Hoshino T: Role of nitric oxide in focal microcirculation disorder of guinea pig cochlea. Hear Res *153*: 7-13, 2001.
13 Takumida M and Anniko M: Lipopolysaccharide-induced expression of nitric oxide synthase II in the guinea pig vestibular end organs. Eur Arch Otorhinolaryngol *255*: 184-188, 1998.
14 Takumida M, Anniko M, Popa R and Zhang DM: Lipopolysaccharide-induced expression of inducible nitric oxide synthase in the guinea pig organ of Corti. Hear Res *140*: 91-8, 2000.

15 Hess A, Bloch W, Huverstuhl J, Su J, Stennert E, Addicks K and Michel O: Expression of inducible nitric oxide synthase (iNOS/NOS II) in the cochlea of guinea pigs after intratympanical endotoxin-treatment. Brain Res *830*: 113-122, 1999.

16 Takumida M, Popa R and Anniko M: Free radicals in the guinea pig inner ear following gentamicin exposure. ORL *61*: 63-70, 1999.

17 Watanabe K, Hess A, Bloch W and Michel O: Expression of inducible nitric oxide synthase (iNOS/NOS II) in the vestibule of guinea pigs after the application of cisplatin. Anticancer Drugs *11*: 29-32, 2000.

18 Hess A, Bloch W, Su J, Stennert E, Addicks K and Michel O: Expression of inducible nitric oxide-synthase in the vestibular system of hydropic guinea pigs. Neurosci Lett *264*: 145-148, 1999.

19 Michel O, Hess A, Su J *et al*: Expression of inducible nitric oxide synthase (iNOS/NOSII) in the hydropic cochlea of the guinea pig. Hear Res *143*: 23-28, 2000.

20 Inafuku S, Wu M, Kimura M, Nakayama M, Nakano T and Ishigami H: Immunohistochemical demonstration of inducible nitric oxide and nuclear factor-kappa B with reference to age-related changes in the mouse spiral and vestibular ganglion. Okajimas Folia Anat Jpn *77*: 125-132, 2000.

21 Watanabe K, Tomiyama S, Jinnouchi K, Pawankar R and Yagi T: Expression of inducible nitric oxide synthase in the cochlea following immune response in the endolymphatic sac of guinea pig. ORL *63*: 155-159, 2001.

22 Takumida M, Anniko M, Popa R and Zhang DM: Pharmacological models for inner ear therapy with emphasis on nitric oxide. Acta Otolaryngol (Stockh) *121*: 16-20, 2001.

23 Kojima H, Sakurai K, Kikuchi K, Kawahara S, Kirino Y, Nagoshi H, Hirata Y and Nagano T: Development of a fluorescent indicator for nitric oxide based on the fluorescein chromophore. Chem Pharm Bull *46*: 373-5, 1998.

24 Kojima H, Nakatsubo N, Kikuchi K, Urano Y, Higuchi T, Tanaka J, Kudo Y and Nagano T: Direct evidence of NO production in rat hippocampus and cortex using a new fluorescent indicator: DAF-2DA. NeuroReport *9*: 3345-8, 1998.

25 Takumida M and Anniko M: Direct evidence of nitric oxide production in guinea pig vestibular sensory cells. Acta Otolaryngol *120*: 34-38, 2000.

26 Takumida M and Anniko M: Direct evidence of nitric oxide production in the guinea pig organ of Corti. Acta Otolaryngol (Stockh) *121*: 342-345, 2001.

27 Sugimoto K, Fujii S, Takemasa T and Yamashita K: Detection of intracellular nitric oxide using a combination of aldehyde fixatives with 4,5-diaminofluorescein diacetate. Histochem Cell Biol *113*: 341-347, 2000.

28 Takumida M and Anniko M: Detection of nitric oxide in the guinea pig inner ear, using a combination of aldehyde fixative and 4,5-diaminofluorescein diacetate. Acta Otolaryngol (Stockh) *121*: 460-464, 2001.

29 Takumida M and Anniko M: Glutamate-induced production of nitric oxide in guinea pig vestibular sensory cells. Acta Otolaryngol *120*: 466-72, 2000.

30 Takumida M and Anniko M: Nitric oxide in guinea pig vestibular sensory cells following gentamicin exposure *in vitro*. Acta Otolaryngol *121*: 346-350, 2001.

31 Tabuchi K, Ito Z, Wada T, Takahashi K, Hara A and Kusakari J: Effect of 7-nitroindazole upon cochlear dysfunction induced by transient local anoxia. Ann Otol Rhinol Laryngol *109*: 715-719, 2000.

32 Heneka MT and Feinstein DL: Expression and function of inducible nitric oxide synthase in neurons. J Neuroimmunol *114*: 8-18, 2001.

33 Brown GC: Regulation of mitochondrial respiration by nitric oxide inhibition of cytochrome c oxidase. Biochim Biophys Acta *1504*: 46-57, 2001.

34 Boczkowski J, Lisdero CL, Lanone S *et al*: Peroxynitrite-mediated mitochondrial dysfunction. Biol Signals Recept *10*: 66-80, 2001.

35 Ohinataab Y, Yamasoba T, Schacht J and Miller JM: Glutathione limits noise-induced hearing loss. Hear Res *146*: 28-34, 2000.

36 Henderson D, McFadden SL, Liu CC, Hight N and Zheng XY: The role of antioxidants in protection from impulse noise. Ann NY Acad Sci *884*: 368-80, 1999.

37 Dehne N, Lautermann J, ten Cate W-JF *et al*: *In vitro* effects of hydrogen peroxide on the cochlear neurosensory epithelium of the guinea pig. Hear Res *143*: 162-170, 2000.

38 Takumida M, Anniko M and Popa R: Possible involvement of free radicals in lipopolysaccharide-induced labyrinthitis. A morphological and a functional investigation. ORL *60*: 246-253, 1998.

39 Popa R, Anniko M and Takumida M: Otoprotectant minimizes hearing defects caused by *Pseudomonas aeruginosa* exotoxin A. Acta Otolaryngol *120*: 350-358, 2000.

40 Watanabe K-I, Hess A, Michel O and Yagi T: Nitric oxide synthase inhibitor reduces the apoptotic change in the cisplatin-treated cochlea of guinea pigs. Anti-Cancer Drugs *11*: 731-735, 2000.

41 Watanabe K, Hess A, Block W and Michel O: Inhibition of inducible nitric oxide synthase lowers the cochlear damage by lipopolysaccharide in guinea pigs. Free Radic Res *13*: 31-37, 2000.

42 Watanabe KI, Hess A, Bloch W and Michel O: Nitric oxide synthase inhibitor suppresses the ototoxic side effect of cisplatin in guinea pig. Anticancer Drugs *11*: 401-406, 2000.

43 Watanabe K, Hess A, Zumeger C *et al*: Changes of the compound action potential (CAP) and the expression of inducible nitric oxide synthase (iNOS/NOS II) in the cochlea under the inflammatory condition. Hear Res *145*: 149-155, 2000.

44 Duan ML, Ulfendahl M, Layrell G, Counter AS, Pyykkö I, Borg E and Rosenhall U: Protection and treatment of sensorineural hearing disorders caused by exogenous factors: experimental findings and potential clinical application. Hear Res *69*: 169-78, 2002.

45 Horner KC and Guilhaume A: Ultrastructural changes in the hydropic cochlea of the guinea pig. Eur J Neurosci *7*: 1305-12, 1995.

46 Shinomori Y and Kimura RS: Allopurinol attenuates endolymphatic hydrops in the guinea pig cochlea. ORL *63*: 267-71, 2001.

47 Takumida M, Anniko M and Ohtani M: Radical scavengers for Meniere's disease after failure of conventional therapy: A pilot study. Acta Otolaryngol *123*: 697-703, 2003.

Received January 28, 2004
Accepted April 2, 2004

Available online at www.sciencedirect.com
SCIENCE DIRECT
Hearing Research 186 (2003) 1–9
HEARING RESEARCH
www.elsevier.com/locate/heares

Bumetanide-induced enlargement of the intercellular space in the stria vascularis critically depends on Na^+ transport

Kasumi Higashiyama, Shunji Takeuchi *, Hiroshi Azuma, Shoichi Sawada, Kazuhiro Yamakawa, Akinobu Kakigi, Taizo Takeda

Department of Otolaryngology, Kochi Medical School, Nankoku 783-8505, Japan

Received 13 January 2003; accepted 8 July 2003

Abstract

The intercellular space in the stria vascularis (intrastrial space) is a closed space and isolated from both the endolymph and the perilymph in normal tissue. Loop diuretics such as bumetanide and furosemide cause an acute enlargement of the intrastrial space in association with a decline in the endocochlear potential. It is known that bumetanide inhibits the Na^+-K^+-$2Cl^-$ cotransporter, which is expressed abundantly in the basolateral membrane of marginal cells. We studied ionic mechanisms underlying the bumetanide-induced enlargement of the intrastrial space using perilymphatic perfusion in guinea pigs. Perilymphatic perfusion with artificial perilymph containing 100 μM bumetanide caused marked enlargement of the intrastrial space, as reported previously. Removal of K^+ from the perilymph did not affect the bumetanide-induced enlargement, whereas removal of Na^+ from the perilymph inhibited it almost completely. Perilymph containing 1 mM amiloride also inhibited the enlargement of the intrastrial space almost completely. These results indicate that perilymphatic Na^+, but not K^+, and amiloride-sensitive pathways are essential to the bumetanide-induced enlargement of the intrastrial space. Two possible pathways could yield these results. Na^+ in the perilymph could enter the endolymph via Reissner's membrane or the basilar membrane; Na^+ in the endolymph would then be taken up by marginal cells via the apical membrane and secreted into the intrastrial space by Na^+-K^+-ATPase in the basolateral membrane of them. Another, less likely possibility is that Na^+ in the perilymph is transported into basal cells or fibrocytes in the spiral ligament, then into intermediate cells via gap junctions, and finally secreted into the intrastrial space via Na^+-K^+-ATPase of intermediate cells.

Key words: Loop diuretic; Na^+-K^+-$2Cl^-$ cotransporter; Amiloride; Perilymph; Endolymph

1. Introduction

The stria vascularis produces the endolymph and the endocochlear DC potential (EP), both of which are essential for the transduction of sound by hair cells (Dallos, 1996). The intercellular space in the stria vascularis (intrastrial space) is unique because it is isolated from both the endolymph and the perilymph by two distinct cell sheets, the marginal cell layer and the basal cell layer, which are connected by tight junctions. It has been proposed that ionic conditions in the intrastrial space are essential for the generation of the EP (Salt et al., 1987; Wangemann and Schacht, 1996; Takeuchi et al., 2000).

Cells constituting the stria vascularis are closely associated and little intrastrial space is observed when normal tissue specimens are examined with transmission electron microscopy. In contrast, loop diuretics such as bumetanide and furosemide cause an acute enlargement of the intrastrial space (Santi and Duvall, 1979; Pike and Bosher, 1980; Santi and Lakhani, 1983) in association with a decline in the EP (Kusakari et al., 1978a,b). Bumetanide inhibits the Na^+-K^+-$2Cl^-$ cotransporter, which is abundantly expressed in the baso-

* Corresponding author. Fax: +81 (88) 880 2395.
E-mail address: kasumi@kochi-ms.ac.jp (S. Takeuchi).

Abbreviations: EP, endocochlear DC potential; NMDG, *N*-methyl-D-glucamine

0378-5955/03/$ – see front matter © 2003 Elsevier B.V. All rights reserved.
doi:10.1016/S0378-5955(03)00226-0

lateral membrane of marginal cells (Crouch et al., 1997; Mizuta et al., 1997). This cotransporter is also expressed in fibrocytes in the spiral ligament (Crouch et al., 1997; Mizuta et al., 1997). There is no doubt that the enlargement of the intrastrial space is caused by the accumulation of solutes, which bring water in osmotically. Because bumetanide disturbs an ion transport mechanism, the solutes accumulating in the enlarged intrastrial space are most likely ions. We have reported that the normal activity of Na^+-K^+-ATPase is required for bumetanide to cause the enlargement of the intrastrial space (Azuma et al., 2002). Accordingly, it is likely that Na^+ or K^+ transported by the Na^+-K^+-ATPase is the major cation accumulating in the enlarged intrastrial space. In this study, we show that Na^+ in the perilymph plays an essential role in the bumetanide-induced enlargement of the intrastrial space.

2. Materials and methods

2.1. Animals and perilymphatic perfusion

Perilymphatic perfusion was performed in essentially the same way as reported previously (Azuma et al., 2002). Briefly, perilymphatic perfusion of both the scala tympani and the scala vestibuli was performed with an inlet at the scala tympani of the basal turn and an outlet at the scala vestibuli of the basal turn. Fifteen albino guinea pigs weighing 260–400 g (SLC, Hamamatsu, Japan) were used in this study. They were anesthetized with ketamine (100 mg/kg, intramuscularly, i.m.) and xylazine (10 mg/kg, i.m.) and artificially ventilated with room air. The left cochlea was exposed by the lateral approach, and both the scala tympani and the scala vestibuli of four cochlear turns were perfused as follows. A fenestration with a diameter of 150–200 μm was made in the bony wall of the scala tympani of the basal turn and the tip of a glass perfusion pipette was inserted into this fenestration. The gap between the perfusion pipette and the fenestrated bony wall was sealed with dental cement to prevent leakage of the perilymph. Perilymphatic perfusion was performed at a flow rate of 10 μl/min using a syringe pump (Nihonkohden CFV3200, Tokyo, Japan) connected to the perfusion pipette. The stapes was dislocated and the artificial perilymph was drained from the oval window.

The control artificial perilymph contained (in mM): NaCl 126, $NaHCO_3$ 24, KCl 5, $CaCl_2$ 1.2, $MgCl_2$ 1, NaH_2PO_4 0.5, and glucose 4 (osmolarity, 290 mOsm/kg). To make K^+-free artificial perilymph, K^+ was replaced by equimolar Na^+. Two kinds of Na^+-free artificial perilymph were used to exclude unknown specific effects of the cations substituted for Na^+. One contained (in mM): choline-Cl 126.5, choline-HCO_3 24, KCl 4.5, $CaCl_2$ 1.2, $MgCl_2$ 1, KH_2PO_4 0.5, glucose 4, and mannitol 11 (osmolarity, 292 mOsm/kg). The other contained (in mM): *N*-methyl-D-glucamine (NMDG) 150, HCl 126, KCl 4.5, $CaCl_2$ 1.2, $MgCl_2$ 1, KH_2PO_4 0.5, glucose 4 (osmolarity, 295 mOsm/kg). Bumetanide was directly dissolved by agitation to a concentration of 100 μM. The artificial perilymph was finally bubbled with a mixture of 95% O_2 and 5% CO_2 for 30 min at 35 ± 1°C (pH 7.4 ± 0.1) and stored in syringes. The total time of perilymphatic perfusion with bumetanide was 40 min.

2.2. Measurement of the EP

We observed changes in the EP to confirm that the perilymphatic perfusion was done properly. The EP levels were recorded from the scala media of the second turn through the lateral wall of the cochlear duct using a glass microelectrode (tip diameter approximately 0.2 μm) filled with 150 mM KCl and connected to an electrometer (FD223, WPI, Sarasota, FL, USA). An Ag-AgCl wire placed in the neck muscle served as a reference. The recording system was zeroed when the pipette tip was placed on the spiral ligament before insertion into the scala media. Voltage drifts were within ± 5 mV when measured with the pipette tip pulled back to the spiral ligament after the experiment had been completed. Data were obtained from animals whose EP was stable at normal levels (> 80 mV) for 6 min under a control condition, i.e. perfusion with the control artificial perilymph.

2.3. Transmission electron microscopy

As soon as perfusion with the experimental solutions was complete, the perilymphatic space was perfused with a phosphate-buffered fixative containing 2.5% glutaraldehyde and 2.0% paraformaldehyde (pH 7.2). The cochlea was removed and the lateral wall of the cochlear duct of the second turn was dissected in the fixative. Tissue strips were immersed in the fixative overnight at 4°C, and then immersed in 1.0% OsO_4 for 60 min at room temperature. After rinsing, the tissue strips were dehydrated in a graded series of ethanol concentrations, stained en block with 2.0% uranyl acetate for 30 min, and embedded in Spurr's resin. Thin sections (90 nm) were made perpendicular to the apical surface of the marginal cells, and stained with uranyl acetate and lead citrate. The sections were examined using an electron microscope (H7100, Hitachi, Japan).

2.4. Quantitative analysis of electron micrographs

Bumetanide-induced changes in the volume of cells and intrastrial space were estimated using the public

domain image processing and analysis program NIH Image (Division of Computer Research and Technology, National Institute of Health, MD, USA) as follows. Three control animals and three bumetanide-treated animals were used. For each animal, three electron micrographs obtained from distinct tissue strips were analyzed. Electron micrographs were converted into digital images composed of 256 gray levels, and then into binary levels of cellular areas and cell-free areas. Segments of the stria vascularis (15–25 μm in width) were analyzed, and cellular areas, cell-free areas in the stria vascularis (i.e. intrastrial spaces), and total areas of the stria vascularis (sum of cellular areas and cell-free areas) per unit width were calculated. Capillaries were omitted from the analysis.

2.5. Data presentation

Data of each experiment were obtained from three animals. Data were presented as mean ± S.D. Data were compared by Student's *t*-test, and differences were regarded as significant when $P < 0.05$. The morphology of the stria vascularis was essentially the same in all animals of each experiment. Thus, representative micrographs from one animal are presented for each experiment.

2.6. Animal care

The care and use of animals used in this study were approved by the Kochi Medical School Animal Care and Use Committee.

3. Results

3.1. Effect of bumetanide

Perilymphatic perfusion with the control artificial perilymph for 90 min did not cause any apparent changes in either the EP or the morphology of the stria vascularis (Fig. 1A–C), as has been reported previously (Azuma et al., 2002). Perilymphatic perfusion for 40 min with the control artificial perilymph containing 100 μM bumetanide caused a decline in the EP from 87.9 ± 3.1 mV to −39.3 ± 13.6 mV and an apparent enlargement of the intrastrial space ($n = 3$) (Fig. 2A–C). In addition, bulging of marginal cells into the scala media

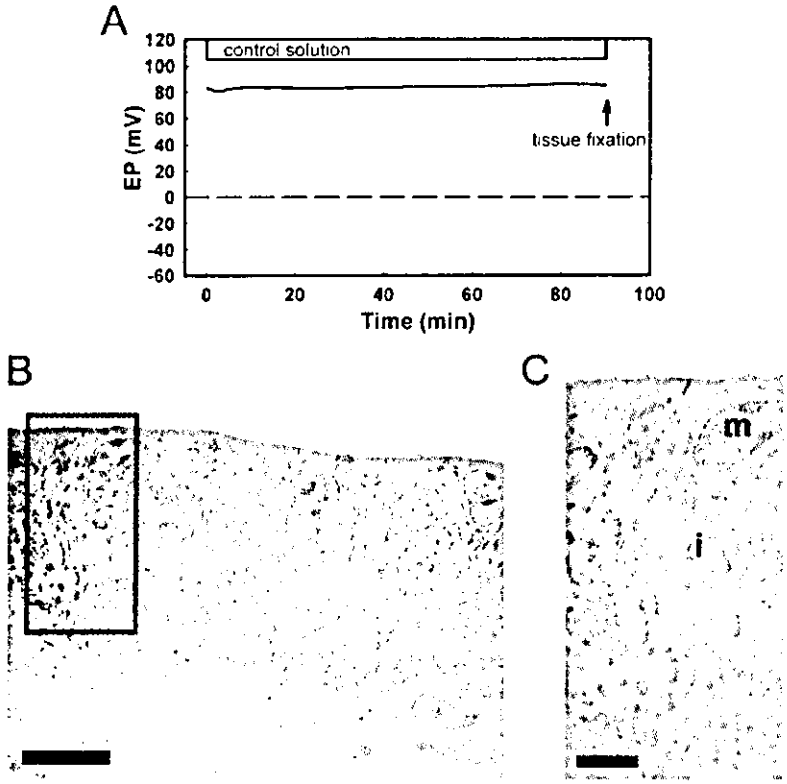

Fig. 1. Effect of control solution on the EP and morphology of the stria vascularis. (A) EP recording during perfusion with control solution. Mean of data from three animals. At the time indicated by the arrow, the strial tissue was chemically fixed by perilymphatic perfusion of fixative. (B) Electron micrograph. Scale bar, 10 μm. (C) Magnification of the rectangular area in B. Scale bar 3 μm. The intrastrial space was not enlarged. m, marginal cell; i, intermediate cell.

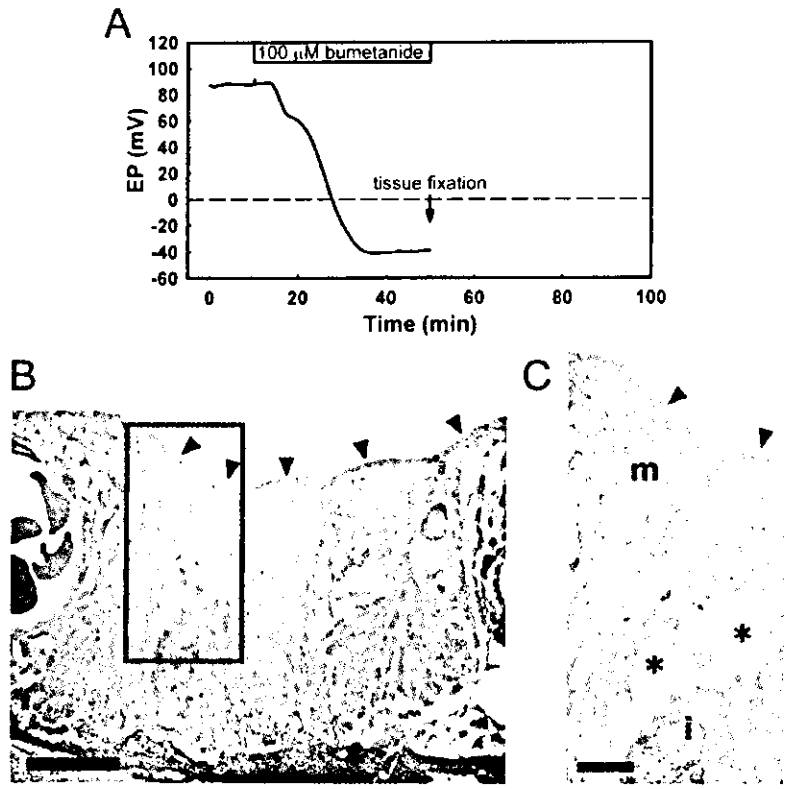

Fig. 2. Effect of bumetanide on the EP and morphology of the stria vascularis. (A) EP recording during perfusion with control solution containing 100 μM bumetanide. Mean of data from three animals. At the time indicated by the arrow, the strial tissue was chemically fixed. (B) Electron micrograph. Scale bar, 10 μm. Note the bulging of apical membrane of marginal cells to the endolymphatic side (arrow heads). (C) Magnification of the rectangular area in B. Scale bar, 3 μm. The intrastrial space was enlarged (asterisks). m, marginal cell; i, intermediate cell.

was observed (Fig. 2C). The morphological change was essentially the same as that reported previously (Azuma et al., 2002).

The difference in the total strial space was not statistically significant between the control animals (33.0 ± 4.1 μm^2/μm) and the bumetanide-treated animals (29.7 ± 5.1 μm^2/μm) (Fig. 3). The difference in the intrastrial space (cell-free areas) was statistically significant between the control animals (0.0 ± 0.0 μm^2/μm) and the bumetanide-treated animals (6.8 ± 2.5 μm^2/μm). The difference in the cellular areas was statistically significant between the control animals (33.0 ± 4.1 μm^2/μm) and the bumetanide-treated animals (22.9 ± 5.4 μm^2/μm). The above results indicate that bumetanide caused an increase in the intrastrial space and a decrease in the cellular volume.

3.2. *Effect of removing K^+ from the perilymph on the bumetanide-induced enlargement of the intrastrial space*

To examine whether K^+ in the perilymph plays an essential role in the enlargement of the intrastrial space, the perilymphatic space was perfused with the K^+-free solution. Perilymphatic perfusion with the K^+-free solution caused a decline in the EP from 83.3 ± 5.3 to -11.9 ± 4.1 mV in 25 min ($n = 3$) (Fig. 4A). Perfusion with the K^+-free solution was continued for 5 min after

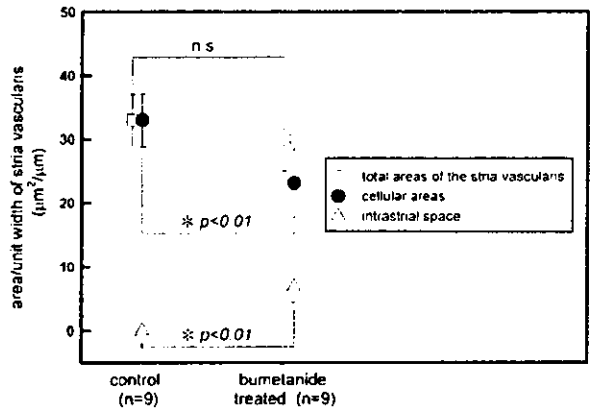

Fig. 3. Quantitative analysis of the changes in the total areas of stria vascularis, cellular areas, and intrastrial space. Areas per unit width of the stria vascularis are plotted. Each data point is based on nine electron micrographs derived from distinct sections. Asterisks, difference is statistically significant; n.s., difference is not statistically significant ($P > 0.05$).

the EP reached a steady value to ensure the removal of K^+ from the perilymph. Then the perilymphatic space was perfused for 40 min with the K^+-free solution containing 100 μM bumetanide. Bumetanide caused the enlargement of the intrastrial space even in the absence of perilymphatic K^+ (Fig. 4B,C). This morphological change was essentially the same as that observed using the control artificial perilymph containing 4.5 mM K^+ and 100 μM bumetanide (Figs. 2B,C).

3.3. Effect of removing Na^+ from the perilymph on the bumetanide-induced enlargement of the intrastrial space

Since K^+ in the perilymph was not essential for the bumetanide-induced enlargement of the intrastrial space, the role of Na^+ in the enlargement of the intrastrial space was examined. Perilymphatic perfusion with the Na^+-free solution containing choline in place of the Na^+ caused a decline in the EP from 86.3 ± 4.9 to 69.0 ± 7.0 mV in 30 min ($n = 3$) (Fig. 5A). Perfusion with the Na^+-free solution was continued for 10 min after the EP reached a steady value. Then the perilymphatic space was perfused for 40 min with the Na^+-free solution containing 100 μM bumetanide. In the absence of Na^+ in the perilymph, bumetanide did not cause the enlargement of the intrastrial space (Figs. 5B,C). Essentially the same results were obtained using another Na^+-free solution in which the Na^+ was replaced with NMDG (n = 3, data not shown).

3.4. Effect of amiloride on the bumetanide-induced enlargement of the intrastrial space

Amiloride is a diuretic drug that blocks subsets of Na^+ transporters such as epithelial Na^+ channels and Na^+-H^+ exchangers. Perilymphatic perfusion with a control solution containing amiloride at 1 mM caused a decline in the EP from 88.6 ± 1.2 to 74.8 ± 11.2 mV in 30 min ($n = 3$) (Fig. 6A). Perfusion for 40 min with a solution containing both 1 mM amiloride and 100 μM bumetanide inhibited the bumetanide-induced enlargement of the intrastrial space almost completely (Figs. 6B,C).

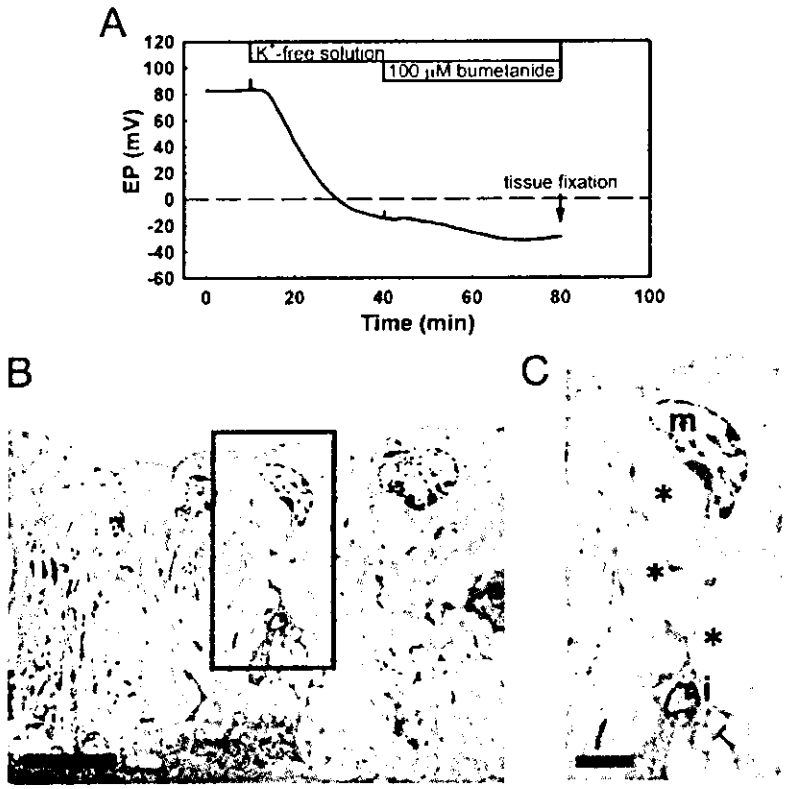

Fig. 4. Effect of K^+ removal from the perilymph. (A) EP recording during perfusion with K^+-free solution. Mean of data from three animals. At the time indicated by the arrow, the strial tissue was chemically fixed. (B) Electron micrograph following perfusion with bumetanide in K^+-free solution. Scale bar, 10 μm. (C) Magnification of the rectangular area in B. Scale bar, 3 μm. Note the enlarged intrastrial space (asterisks). m, marginal cell; i, intermediate cell.

4. Discussion

4.1. Structural consideration of the intrastrial space

The intrastrial space is a closed space and is isolated from both the endolymph and the perilymph. Two kinds of plasma membrane face the intrastrial space, the basolateral membrane of marginal cells and the syncytium, which is composed of intermediate cells, basal cells, fibrocytes of the spiral ligament, and cells constituting capillaries, all connected by gap junctions (Takeuchi et al., 2000). In the basolateral membrane of the marginal cells, Na^+-K^+-ATPase, Na^+-K^+-$2Cl^-$ cotransporters, and Cl^- channels are expressed abundantly (Kerr et al., 1982; Schulte and Adams, 1989; Crouch et al., 1997; Mizuta et al., 1997; Takeuchi et al., 1995; Takeuchi and Irimajiri, 1996). Intermediate cells are the major component of the syncytium and express K^+ channels abundantly (Ando and Takeuchi, 1999; Takeuchi and Ando, 1999). The Na^+-K^+-$2Cl^-$ cotransporter, which is inhibited by bumetanide, is expressed not only in the basolateral membrane of marginal cells but also in type II and V fibrocytes in the spiral ligament (Crouch et al., 1997; Mizuta et al., 1997; Weber et al., 2001). As the basolateral membrane of marginal cells faces the intrastrial space, the major site of bumetanide action related to the enlargement of the intrastrial space is likely to be the basolateral membrane of marginal cells. Although we administered bumetanide to the perilymph, bumetanide is expected to reach the basolateral membrane of marginal cells across the basal cell layer because it is a lipophilic agent. Solutes, most likely ions, are probably transported across the plasma membranes facing the intrastrial space and accumulate in this space.

4.2. Na^+ transport and the bumetanide-induced enlargement of the intrastrial space

The bumetanide-induced enlargement of the intrastrial space requires not only the blockade of Na^+-K^+-$2Cl^-$ cotransporter but also the normal activity of Na^+-K^+-ATPase (Azuma et al., 2002). This study has further revealed that perilymphatic Na^+, but not K^+, is essential to the enlargement of the intrastrial space (Figs. 4 and 5). In general, the stoichiometry of Na^+-K^+-ATPase is $3Na^+/2K^+$, and Na^+ is pumped out of cells. We therefore speculate that Na^+ is extruded from

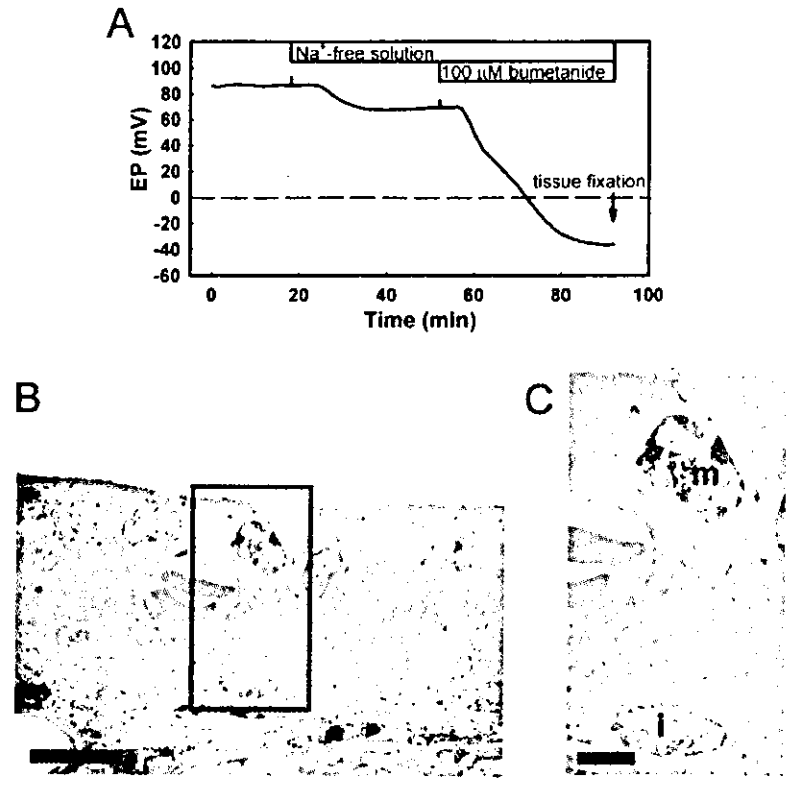

Fig. 5. Inhibition of the bumetanide-induced enlargement of the intrastrial space by removal of perilymphatic Na^+ (choline substitution) from both the scala tympani and scala vestibuli. (A) EP recording during perfusion with Na^+-free solution. Mean of data from three animals. At the time indicated by the arrow, the strial tissue was chemically fixed. (B) Electron micrograph. Scale bar, 10 μm. (C) Magnification of the rectangular area in B. Scale bar, 3 μm. The intrastrial space was not enlarged. m, marginal cell; i, intermediate cell.

the inside of marginal cells and accumulates in the intrastrial space when Na^+ uptake via the Na^+-K^+-$2Cl^-$ cotransporter is blocked by bumetanide.

The Na^+-K^+-ATPase activity in the basolateral membrane of marginal cells is high (Kerr et al., 1982; Schulte and Adams, 1989), and its physiological role has been generally accepted to be taking up K^+ from the intrastrial space and keeping the intracellular Na^+ concentration low. The low intracellular Na^+ concentration provides a driving force for the Na^+-K^+-$2Cl^-$ cotransporter. We speculate that the Na^+-K^+-ATPase in the basolateral membrane of marginal cells plays a major role in the bumetanide-induced enlargement of the intrastrial space (although it cannot be excluded that Na^+ enters basal cells or fibrocytes in the spiral ligament, is transported to intermediate cells via gap junctions, and is then secreted into the intrastrial space via Na^+-K^+-ATPase in intermediate cells). It is expected that anions also accumulate in the intrastrial space to maintain electrical neutrality, and that Na^+ and associated anions (most likely Cl^- and HCO_3^-) cause the osmotic movement of water.

The electrochemical gradient for Na^+ under physiological conditions is directed from the perilymph to the endolymph by approximately 30–40 mV assuming that the Na^+ concentrations in the perilymph and the endolymph are 150 and 1.5 mM respectively, and that the EP is 80–90 mV. Accordingly, it is expected that Na^+ flux into the endolymph may occur under physiological conditions (a in Fig. 7A). When the EP decreases as a result of bumetanide effects, the electrochemical gradient for Na^+ flux into the endolymph is expected to increase (a′ in Fig. 7B). This may enhance the Na^+ entry into the marginal cells, and the enlargement of the intrastrial space.

4.3. *Possible route of Na^+ transport from the perilymph to the intrastrial space*

The route of Na^+ transport from the perilymph to the intrastrial space is not yet entirely clear. One possibility is that Na^+ in the perilymph enters the endolymph via Reissner's membrane or structures on the basilar membrane including the organ of Corti, then Na^+ in the endolymph is taken up by marginal cells via their apical membranes, and finally Na^+ in the marginal cells is then secreted into the intrastrial space by Na^+-K^+-ATPase in the basolateral membrane (a in Fig. 7A). It is likely that this Na^+ transport pathway plays an important role in maintaining the low Na^+ concen-

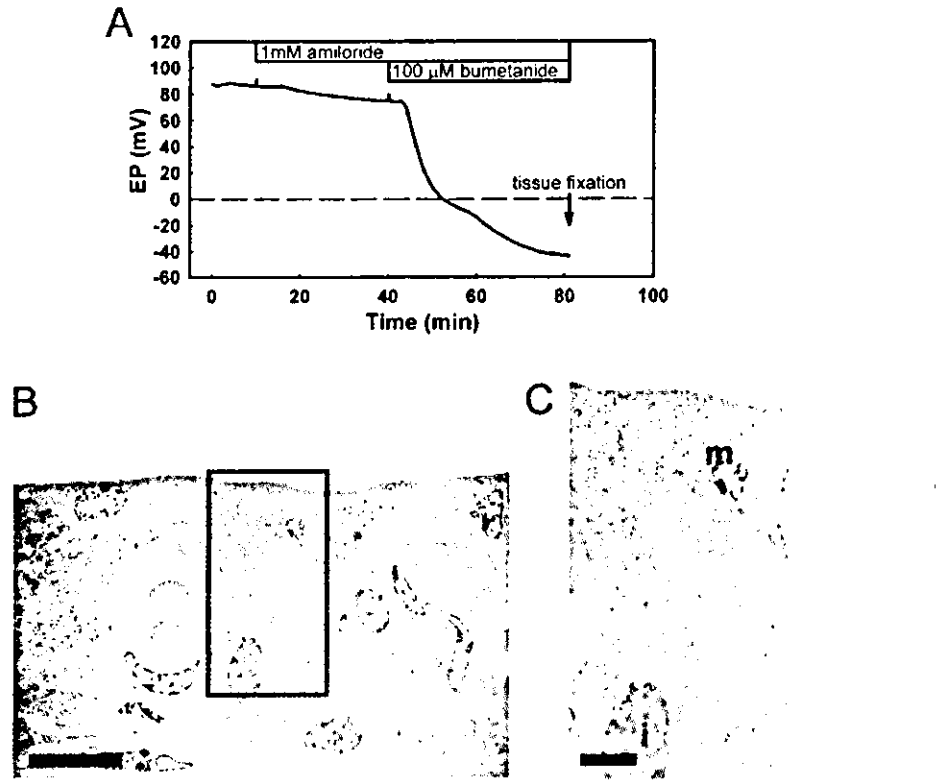

Fig. 6. Inhibition of the bumetanide-induced enlargement of the intrastrial space by amiloride. (A) EP recording during perfusion with control solution containing 1 mM amiloride. Mean of data from three animals. At the time indicated by the arrow, the strial tissue was chemically fixed. (B) Electron micrograph. Scale bar, 10 μm. (C) Magnification of the rectangular area in B. Scale bar, 3 μm. Amiloride at 1 mM almost completely inhibited the bumetanide-induced enlargement of the intrastrial space. m, marginal cell; i, intermediate cell.

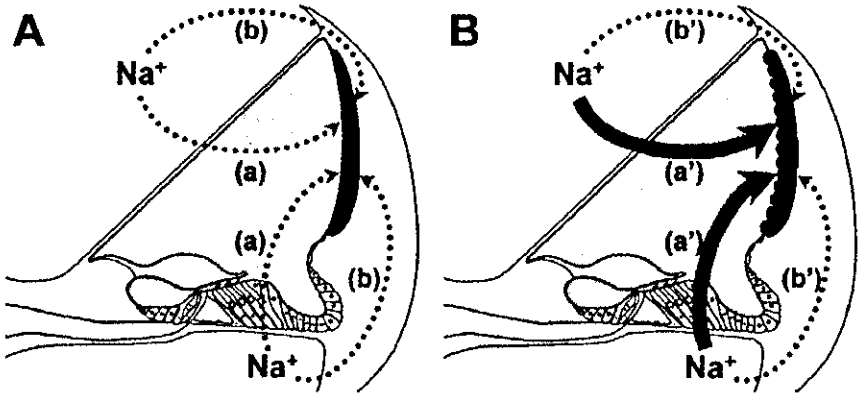

Fig. 7. Possible routes of Na^+ transport from the perilymph to the intrastrial space. (A) Na^+ transport under physiological conditions. a, Na^+ in the perilymph enters the endolymph via Reissner's membrane and/or structures on the basilar membrane including the organ of Corti, then Na^+ in the endolymph is taken up by marginal cells via the apical membrane, and finally secreted into the intrastrial space. b, Na^+ in the perilymph is transported from basal cells or fibrocytes in the spiral ligament to intermediate cells via gap junctions and secreted into the intrastrial space. (B) Na^+ transport under the effect of bumetanide. When the EP decreased as a result of bumetanide administration, the electrochemical gradient for Na^+ flux from the perilymph to the endolymph increases (a').

tration in the endolymph under physiological conditions.

Amiloride blocks not only amiloride-sensitive Na^+ channels but also the Na^+/H^+ exchanger. Amiloride-sensitive Na^+ channels are expressed in the stria vascularis (Couloigner et al., 2001), and are possibly expressed in the apical membrane of marginal cells (Mizuta et al., 1995). The Na^+/H^+ exchanger is expressed in the apical membrane of marginal cells (Bond et al., 1998). In view of the reports mentioned above and our results that amiloride inhibited the bumetanide-induced enlargement of the intrastrial space (Figs. 6B,C), amiloride may inhibit Na^+ transport from the endolymph into marginal cells via amiloride-sensitive Na^+ channels and/or the Na^+/H^+ exchanger in the apical membrane of marginal cells. Nonselective cation channels in the apical membrane of marginal cells (Takeuchi et al., 1995) may also provide a route for Na^+ transport from the endolymph to marginal cells.

Functional expression of the Na^+/H^+ exchanger in the basolateral membrane of marginal cells has also been reported (Wangemann et al., 1996). However, it is questionable that this transporter in this particular location contributes to the enlargement of the intrastrial space as this transporter is expected to transport Na^+ from the extracellular side to the intracellular side (i.e. from the intrastrial space to the inside of marginal cells) when usual electrophysiological gradients for Na^+ and H^+ are assumed.

As mentioned in the previous section, it is also possible that Na^+ in the perilymph is transported into basal cells or fibrocytes in the spiral ligament, then into intermediate cells via gap junctions, and finally secreted into the intrastrial space via Na^+-K^+-ATPase of intermediate cells (b in Fig. 7A). In this case, the amiloride-sensitive transporter might be present in fibrocytes and/or basal cells. However, this is less likely since the activity of Na^+-K^+-ATPase in intermediate cells is thought to be lower than that in marginal cells.

It is unlikely that the Na^+ in the blood plasma in the strial capillaries accumulates in the intrastrial space since normal blood plasma, containing a high concentration of Na^+, was present in strial capillaries when the enlargement of the intrastrial space was suppressed by Na^+ removal from the perilymph (Figs. 5B,C).

4.4. Shrinkage of cells caused by bumetanide

In association with the enlargement of the intrastrial space, shrinkage of cells in the stria vascularis occurred (Fig. 3). As bumetanide inhibits Na^+-K^+-$2Cl^-$ cotransporter, a decrease in the solute uptake by marginal cells via this cotransporter might be a major cause of the bumetanide-induced cell shrinkage. It is unlikely that cell shrinkage caused the bulging of the apical membrane of marginal cells (Figs. 2B,C). We speculate that accumulation of solutes and water in the intrastrial space caused a shift of marginal cells to the endolymphatic side.

4.5. Relation to the K^+-recycling mechanism in the cochlea

Although K^+ is not the cation that accumulates in the enlarged intrastrial space (Fig. 4B,C), this result does not refute the K^+-cycling theory, which asserts that K^+ in the perilymph is taken up by fibrocytes in the spiral ligament, transported via gap junctions to basal cells and intermediate cells, and then secreted into the intrastrial space (Spicer and Schulte, 1996;

Wangemann, 2002). Rather, the importance of perilymphatic K^+ for the generation of the EP was demonstrated in a previous report (Marcus et al., 1981) and confirmed in this study (Fig. 4A).

Acknowledgements

The authors thank Mr. Ken-ichi Yagyu and Ms. Aya Uchida for technical assistance. This study was supported by a Grant-in-Aid for Scientific Research (C) from The Ministry of Education, Culture, Sports, Science and Technology, Japan (#12671671).

References

Ando, M., Takeuchi, S., 1999. Immunological identification of an inward rectifier K^+ channel (Kir4.1) in the intermediate cell (melanocyte) of the cochlear stria vascularis of gerbils and rats. Cell Tissue Res. 298, 179–183.

Azuma, H., Higashiyama, K., Takeuchi, S., Ando, M., Kakigi, A., Nakahira, M., Yamakawa, K., Takeda, T., 2002. Bumetanide-induced enlargement of the intercellular space in the stria vascularis requires an active Na^+-K^+-ATPase. Acta Otolaryngol. 122, 816–821.

Bond, B.R., Ng, L.L., Schulte, B.A., 1998. Identification of mRNA transcripts and immunohistochemical localization of Na/H exchanger isoforms in gerbil inner ear. Hear. Res. 123, 1–9.

Couloigner, V., Fay, M., Djelidi, S., Farman, N., Escoubet, B., Runembert, I., Sterkers, O., Friedlander, G., Ferrary, E., 2001. Location and function of the epithelial Na channel in the cochlea. Am. J. Physiol. Renal Physiol. 280, F214–F222.

Crouch, J.J., Sakaguchi, N., Lytle, C., Schulte, B.A., 1997. Immunohistochemical localization of the Na-K-Cl co-transporter (NKCC1) in the gerbil inner ear. J. Histochem. Cytochem. 45, 773–778.

Dallos, P., 1996. Overview: Cochlear Neurobiology. In: Dallos, P., Popper, A.N., Fay, R. (Eds.), Springer Handbook of Auditory Research, Vol. 8: The Cochlea. Springer, Berlin, pp. 1–43.

Kerr, T.P., Ross, M.D., Ernst, S.A., 1982. Cellular localization of Na^+,K^+-ATPase in the mammalian cochlear duct: significance for cochlear fluid balance. Am. J. Otolaryngol. 3, 332–338.

Kusakari, J., Ise, I., Comegys, T.H., Thalmann, I., Thalmann, R., 1978a. Effect of ethacrynic acid, furosemide, and ouabain upon the endolymphatic potential and upon high energy phosphates of the stria vascularis. Laryngoscope 88, 12–37.

Kusakari, J., Kambayashi, J., Ise, I., Kawamoto, K., 1978b. Reduction of the endocochlear potential by the new 'loop' diuretic bumetanide. Acta Otolaryngol. 86, 336–341.

Marcus, D.C., Marcus, N.Y., Thalmann, R., 1981. Changes in cation contents of stria vascularis with ouabain and potassium-free perfusion. Hear. Res. 4, 149–160.

Mizuta, K., Adachi, M., Iwasa, K.H., 1997. Ultrastructural localization of the Na-K-Cl cotransporter in the lateral wall of the rabbit cochlear duct. Hear. Res. 106, 154–162.

Mizuta, K., Iwasa, K.H., Tachibana, M., Benos, D.J., Lim, D.J., 1995. Amiloride-sensitive Na^+ channel-like immunoreactivity in the luminal membrane of some non-sensory epithelia of the inner ear. Hear. Res. 88, 199–205.

Pike, D.A., Bosher, S.K., 1980. The time course of the strial changes produced by intravenous furosemide. Hear. Res. 3, 79–89.

Salt, A.N., Melichar, I., Thalmann, R., 1987. Mechanisms of endocochlear potential generation by stria vascularis. Laryngoscope 97, 984–991.

Santi, P.A., Duvall, A.J., III, 1979. Morphological alteration of the stria vascularis after administration of the diuretic bumetanide. Acta Otolaryngol. 88, 1–12.

Santi, P.A., Lakhani, B.N., 1983. The effect of bumetanide on the stria vascularis: a stereological analysis of cell volume density. Hear. Res. 12, 151–165.

Schulte, B.A., Adams, J.C., 1989. Distribution of immunoreactive Na^+,K^+-ATPase in gerbil cochlea. J. Histochem. Cytochem. 37, 127–134.

Spicer, S.S., Schulte, B.A., 1996. The fine structure of spiral ligament cells relates to ion return to the stria and varies with place-frequency. Hear. Res. 100, 80–100.

Takeuchi, S., Ando, M., 1999. Voltage-dependent outward K^+ current in intermediate cell of stria vascularis of gerbil cochlea. Am. J. Physiol. 277, C91–C99.

Takeuchi, S., Irimajiri, A., 1996. A novel, volume-correlated Cl^- conductance in marginal cells dissociated from the stria vascularis of gerbils. J. Membr. Biol. 150, 47–62.

Takeuchi, S., Ando, M., Kakigi, A., 2000. Mechanism generating endocochlear potential: role played by intermediate cells in stria vascularis. Biophys. J. 79, 2572–2582.

Takeuchi, S., Ando, M., Kozakura, K., Saito, H., Irimajiri, A., 1995. Ion channels in basolateral membrane of marginal cells dissociated from gerbil stria vascularis. Hear. Res. 83, 89–100.

Wangemann, P., 2002. K^+ cycling and the endocochlear potential. Hear. Res. 165, 1–9.

Wangemann, P., Schacht, J., 1996. Homeostatic Mechanisms in the Cochlea. In: Dallos, P., Popper, A.N., Fay, R. (Eds.), Springer Handbook of Auditory Research, Vol. 8: The Cochlea. Springer, Berlin, pp. 130–185.

Wangemann, P., Liu, J., Shiga, N., 1996. Vestibular dark cells contain the Na^+/H^+ exchanger NHE-1 in the basolateral membrane. Hear. Res. 94, 94–106.

Weber, P.C., Cunningham, C.D., III, Schulte, B.A., 2001. Potassium recycling pathways in the human cochlea. Laryngoscope 111, 1156–1165.